UDC 539.4

Analysis and Experimental Study of Vibration System Characteristics of Ultrasonic Compound Electrical Machining

Z. Q. Deng, Y. W. Zhu,[1] F. Wang, X. Gu, and D. Yang

Collage of Mechanical Engineering, Yangzhou University, Yangzhou, China

[1] ywzhu@yzu.edu.cn

The effect of applying ultrasonic vibration in the ultrasonic compound electrical machining is analyzed. According to the resonance system during machining and on the basis of vibration theory, the shape and dimension parameters of the ultrasonic amplitude transformer and the tool head are calculated and analyzed. The amplitude transformer and the tool head used in this experiment have been designed to meet the requirements of this investigation. Under different conditions, ultrasonic vibration parameters are measured online using the high-speed high-precision micro-displacement laser sensor. The obtained results show high accuracy and efficiency of the investigation. The relationship parameters between the ultrasound amplitude and the ultrasonic excitation voltage are obtained from the mathematical calculations. The results provide the basic conditions for online optimization of the ultrasonic compound electrical machining parameters. Meanwhile, the working stability of the ultrasonic vibration system and the technical advantages of the ultrasonic compound electrical machining method are verified using the analysis results. In order to do this, the processing parameters have been reasonably selected, while the ultrasound machining and ultrasonic compound electric machining have been tested on ceramics, carbide, and other hard yet brittle materials.

Keywords: ultrasound modulation, ultrasound machining, compound electric machining, vibration characteristic, online measurement.

Introduction. Ceramics, optical glass, functional crystals, diamonds, gems and other advanced compound materials exhibit excellent physical, chemical, and mechanical properties. With this in view, these materials are widely used in fields such as aviation, aerospace, defense, electronics, automobile manufacturing, and bio-engineering. The key to rapid development in these areas (and others) is to discover how to achieve high-precision, high-efficiency, and high-reliability processing of these materials [1].

Ultrasonic compound electrical machining involves cavitations, pumping, vortex action, micro spark discharge, electrochemical reaction, and other effects. A number of experiments and theoretical interventions proved that this kind of machining is efficient when working with hard, brittle, difficult-to-process materials [2].

Shabgard and Alenabi [3] proposed to perform the electrochemical machining assisted by electrode ultrasonic vibrations with single-ended insulated electrodes. This is the method that can potentially enhance the process stability and facilitate the generation of sparks, thereby increase the machining depth. Shao et al. [4] carried out the processing speed craft comparative test on the ultrasonic compound EDM (electrical discharge machining) using the different electrical and electrode parameters. He found that the cut-off point is 3 mm in machining the diameter of holes independent of the use of ultrasonic EDM. Chen and Lin [5] studied the machining of complex surfaces using the ultrasound compound EDM forming and pulse electrochemical compound mechanical polishing. A uniform surface finish is achieved by applying the finishing tool, moreover, this method can ensure stable EDM with small discharge energy. In this case, the profile surface roughness is reduced, and the surface is machined to the mirror-like one [6].

The results of the ultrasonic compound electric machining reveal that due to load change in the ultrasonic vibration system, transducer heating, and tool head wear, the

stability of the machining status is found to be difficult to maintain during machining [7]. Ultrasonic vibration amplitude is the important factor that affects the efficiency of ultrasound compound electrical machining. For instance, the larger vibration amplitude can ensure a certain processing speed and exclude processed products. This is currently the basis for setting the power gap [8, 9]. In this paper, the laser displacement sensor for detecting the amplitude is used to analyze the relationship between the vibration amplitude and the excitation voltage.

1. **Analysis and Design of Ultrasonic Vibration System**. The ultrasonic vibration system is the core section of the ultrasonic compound electric machining equipment. The equipment tool end surface possess a relatively high velocity or displacement amplitude, but the amplitude of the ultrasonic transducer end is generally of 1~10 μm. Therefore, the ultrasonic transducer cannot meet the requirements of machining. It requires the increase of access level and/or two amplitude transformers on the front face of the transducer to augment the amplitude [10]. The ultrasonic vibration system usually consists of the transducer, the amplitude transformer, and the tool head. These three elements are analyzed in detail in the following section.

1.1. ***Transducer***. The piezoelectric ceramic transducer is manufactured based on the inverse piezoelectric effect of the piezoelectric crystal, since crystal exhibits higher electro acoustical efficiency, and it has a simple structure. For the vibration transducer of sheet thickness in the quasi-static case, piezoelectric equation can be expressed as [11]:

$$\gamma = \varepsilon t = d_{33} U,$$

where γ is the displacement, ε is the strain, d_{33} is the piezoelectric constant, U is the transducer terminal voltage, and t is the thickness. As the equation above shows, there is a positive correlation between the displacement of the piezoelectric transducer and the applied voltage.

For the piezoelectric sandwich transducer selected in this paper, the setting conditions were as follows: the piezoelectric ceramic material was PZT-4 launch of the ceramic sheet, it consisted of six pieces, thickness was 8 mm, beryllium bronze pieces were used as electrodes, the rear cover was 45 steel, and the front cover was aluminum alloy. The final shape of the structure is illustrated in Fig. 1.

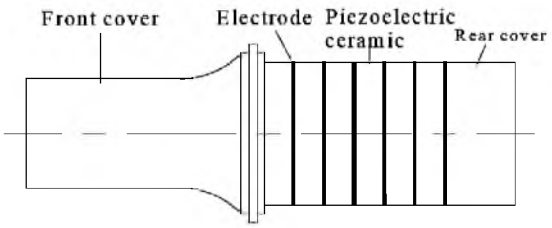

Fig. 1. Schematic diagram of piezoelectric sandwich transducer.

1.2. ***Amplitude Transformer***. The main function of the ultrasonic amplitude transformer is to amplify the mechanical vibration and/or particle velocity. Ultrasonic energy can also be concentrated in the smaller area, in that case it is the spot energy.

For variable cross sections of the vibration amplitude transformer, assuming that the variable cross bar is taken from the homogeneous isotropic material and excluding the mechanical loss conditions, the wave equation is as follows [12]:

$$\frac{\partial^2 \xi}{\partial x^2} + \frac{1}{S}\frac{\partial S}{\partial x}\frac{\partial \xi}{\partial x} + k^2 \xi = 0, \tag{1}$$

where $k = w/c$ is the circular wave number (w is circular frequency and c is the longitudinal wave velocity), x is the coordinate of the rod cross section, $S = S(x)$ is the area function, and ξ is the amplitude transformer displacement.

For the exponential transformer, the area functions are

$$S = S_1 e^{-2\beta x}, \tag{2}$$

where β is the meandering index, $\beta = \ln N / l_1$, l_1 is the length of the exponential transformer, N is the area factor, $N = D_1/D_2$, D_1, S_1, D_2 are the big-end and small-end diameters. Merging Eq. (2) into Eq. (1), we obtain the general solution for displacement section in the exponential transformer:

$$\xi_1 = e^{\beta x}[A_1 \cos k_1 x + B_1 \sin k_1 x].$$

For the stepped amplitude transformer, the area function is as follows:

$$\begin{cases} S = S_3 & (-a \le x \le 0), \\ S = S_4 & (0 < x \le b), \end{cases} \tag{3}$$

where S_3 and S_4 are the cross sections of thick and thin areas, respectively, a denotes the length of the thick section and b denotes the length of the fine section. Inserting them into Eq. (1), the general solution of the stepped amplitude transformer sectional displacement can be expressed as

$$\begin{cases} \xi_3 = A_3 \cos kx + B_3 \sin kx & (-a \le x \le 0), \\ \xi_4 = A_4 \cos kx + B_4 \sin kx & (0 < x \le b). \end{cases}$$

Consequently, these conditions can be used to derive the formulas shown in Table 1.

T a b l e 1

Design Formulas of Amplitude Transformer

Parameter	Exponential transformer	Stepped amplitude transformer
Frequency equation	$\sin(k_1 l_1) = 0$	$S_3 \tan ak + S_4 \tan bk = 0$
Resonant length of half-wavelength	$l_1 = \frac{\lambda}{2}\sqrt{1 + \left(\frac{\ln N}{\pi}\right)^2}$	$l_2 = a + b = \frac{\lambda}{2}$
Displacement node	$x_{01} = \frac{l_1}{\pi} \operatorname{arccot}\left(\frac{\ln N}{\pi}\right)$	$x_{02} = b - \frac{\lambda}{4}$
Magnification factor	$M_1 = \left\|\frac{\xi_2}{\xi_1}\right\| = e^{\beta l_1}\left(\cos k_1 l_1 - \frac{\beta}{k_1}\sin k_1 l_1\right) = N$	$M_2 = \frac{S_3}{S_4}\frac{\sin ka}{\sin kb}$
Strain maximum points	$x_M = \frac{1}{k_1}\arctan\left(-\frac{k_1}{\beta}\right)$	
Form factor	$\varphi_1 = N\frac{k_1}{k} e^{-\beta x_M} \frac{1}{\sin(k_1 x_M)}$	In theory, form factor: $\varphi_2 = 1$, whereas in actuality, $\varphi_2 < 0.8$.

In this experiment, the amplitude transformer was made of 45 quenched and tempered steel. The working frequency was 20 kHz and the longitudinal wave velocity was $c =$ $= 5170$ m/s. The big-end and small-end diameters of the amplitude transformers were 30 and 16 mm, respectively.

As seen in Table 1, the exponential amplitude transformer parameters are as follows: the resonant length of half-wavelength, $l_1 = 132$ mm, and the magnification factor, $M_1 = 1.875$. The displacement node was $x_{01} = 57.7$ mm and the strain maximum point was $x_M = 74.3$ mm. Figure 2a and 2b shows, the transformer dimensions for factor $\varphi_1 = 1.31$ and its general view, respectively,.

From Table 1 is evident that the stepped amplitude transformer parameters are as follows: the resonant length of half-wavelength is $l_2 = 129.25$ mm, $a = 20$ mm, $b = 109.25$ mm, and $Ra = 7.68$ mm (corner radius). The magnification factor is $M_2 = 3.64$, whereas the displacement node is $x_{02} = 44.375$ mm. The form factor $\varphi_2 = 1$ and its overall dimensions are given in Fig. 2c and 2d, respectively.

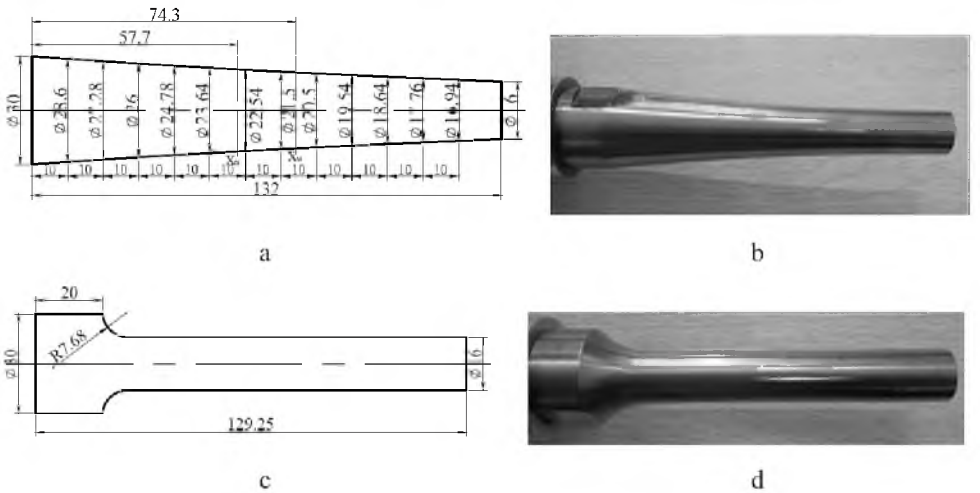

Fig. 2. Ultrasonic transformer: (a) overall dimension of the exponential amplitude transformer (unit: mm); (b) exponential amplitude transformer; (c) overall dimension of the stepped amplitude transformer (unit: mm); (d) stepped amplitude transformer.

1.3. ***Tool Head***. During the ultrasonic compound electric machining, the tool head must be connected to the amplitude transformer small head in order to perform the efficient machining. The transformer structure, size, quality, and connection status have a great effect on both the ultrasonic vibration resonance frequency and the working performance [13, 14].

In this study, the circular hole-shaped tool head is used (Fig. 3). The front end surface of this head is smooth, which improves the focus of the laser displacement sensor. After brushing vaseline on the front end, the faying surface was fastened with bolts and threads.

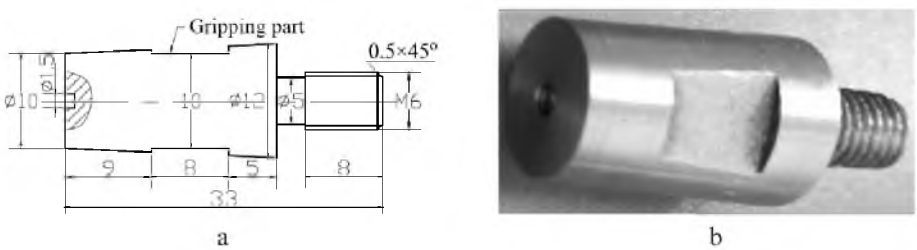

Fig. 3. Tool head circular hole: (a) tool head overall dimensions (unit: mm); (b) tool head.

2. **Measurement and Analysis**. Based on above mentioned, the maximum amplitude value that an ultrasonic vibration system can achieve is related to the design of each of its structural parts. However, in practice, the ultrasonic compound electric machining, the input voltage and the installation of the tool head on the amplitude transformer are the main factors that have a drastic effect on the ultrasonic vibration system output amplitude. Moreover, this occurs when the system is adjusted to the resonance conditions.

2.1. ***Amplitude Method and Voltage Measurement***. Figure 4 presents the schematic diagram of the ultrasonic amplitude and voltage measurement, as well as the transformer and small-end tool head amplitudes measured by the LK-G5000 laser displacement sensor (produced by Keyence). The measurement accuracy of this type of laser displacement sensor can attain the value of 0.01 μm. This sensor can also have the sampling frequency of up to 392 KHz, which is twice higher than the value attained by the ultrasonic vibration system. In the process of testing, the voltage transmitter is placed parallel to the ultrasonic power supply voltage output port, and then the voltage applied to the piezoelectric ceramic stack at both ends is measured. Using the Advantech PCI-1706U data acquisition card, the voltage transducer output signal is converted and then recorded by the computer. The analysis is performed, and the data is displayed at the LabVIEW software platform. Figure 5 illustrates the field test.

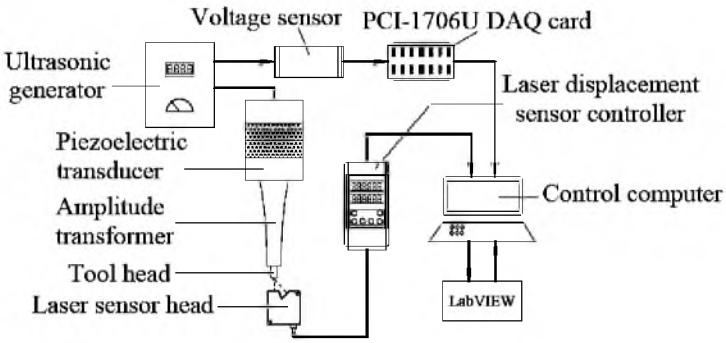

Fig. 4. Ultrasonic amplitude and voltage measurement.

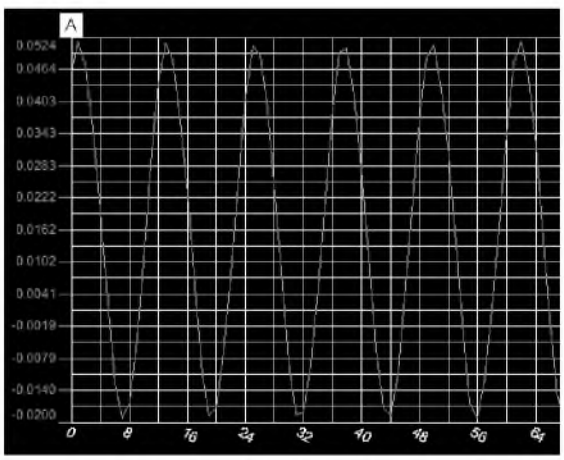

Fig. 5. Ultrasonic amplitude curve measured by laser sensor.

2.2. ***Amplitude Transformer Test without the Tool Head***. When the small end of the amplitude transformer is not connected to the tool head, the output terminal is free. Here is observed that the stepped amplitude transformer actual vibration frequency was 17.4 kHz,

while the exponential amplitude transformer frequency was 18.3 kHz. After processing, the ultrasonic power supply voltage was gradually increased from 20 V to the maximum voltage. The real-time variation of the voltage value was observed in the LabVIEW waveform acquisition window. Laser displacement sensor control software was used to measure the amplitude value at the intervals of 12 V.

As is seen from Fig. 6 with an increase in the transducer input voltage, the amplitude value of the transformer small end also increases. Aligning the smallest squares linear fit with the experimental data from LabVIEW and using fitting parameters including amplitude and input voltage allow one to obtain the relationship with amplitude (A) and voltage (U).

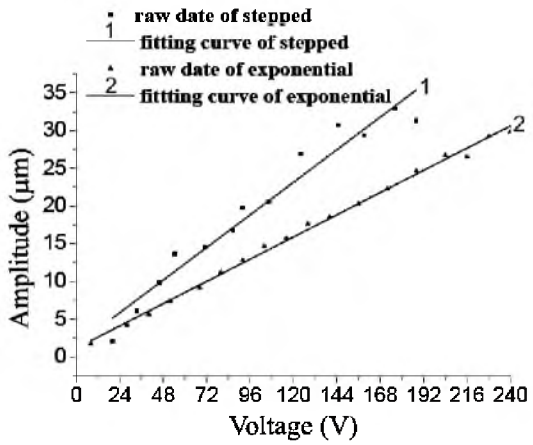

Fig. 6. Amplitude and voltage variations without tool.

The formula for the stepped amplitude transformer amplitude and input voltage:

$$A_1 = 0.176U + 0.457.$$

The formula for the exponential amplitude transformer amplitude and input voltage:

$$A_2 = 0.124U + 0.955.$$

2.3. ***Amplitude Transformer with the Tool Head***. As it was found, the tool head shape and dimensions determine the shape and the dimensions of the workpiece forming surface, and the difference (if any) in the working space (slightly larger than the average diameter of the abrasive particles). The tool head longitudinal length used in this experiment was less than 1/10 of the wavelength, thus, the quality impact on vibration can be neglected.

At the outset, the single-point measurement method was used, and then the frequency point was adjusted at the maximum input power. Then, the ultrasonic power excitation capacitors were changed and used to measure the relationship between the ultrasonic amplitude and the frequency adjustment point. Finally, the system resonance frequency was determined.

When the ultrasonic amplitude transformer material and size were determined, the resonant frequency of the amplitude transformer was not fixed, but varied according to the load impedance. For instance, with an inductive load for the tool head the resonant frequency would be declined.

Using the laser displacement sensor to measure the corresponding amplitude followed by the gradual increase of the ultrasound input voltage allows one to obtain the correlation between the amplitude and the input voltage (Fig. 7).

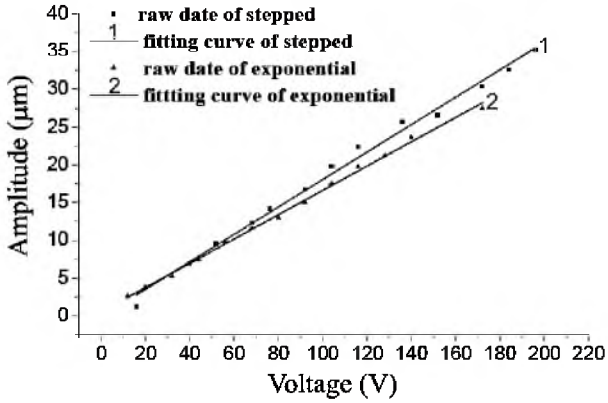

Fig. 7. Amplitude and voltage variations with tool head.

The fitting formula for the stepped amplitude transformer amplitude and input voltage:

$$A_3 = 0.179U + 0.134.$$

The fitting formula for the exponential amplitude transformer amplitude and input voltage:

$$A_4 = 0.163U + 0.412.$$

According to the ultrasonic machining, here the power of the ultrasonic generator is used to convert the mechanical energy of the tool head vibration. The strength of the vibration energy can be used to measure the energy density J [15]:

$$J = \frac{1}{2}\rho c(wA)^2 = \frac{P}{S} = \frac{U^2}{RS}, \tag{4}$$

where ρ is elastic medium density, P is the power, and R is the resistance. Equation (4) shows that $A \propto U$.

Comparison of the maximum amplitude value of the ultrasonic vibration system output end face, independent of whether the tool head is connected (or not) made it possible to conclude that the maximum amplitude value was increased for both the stepped amplitude transformer and exponential transformer. This is due to the resonance of the amplitude transformer–tool system combination, and to the design tool head smaller mass and smaller sectional dimension as compared with the amplitude transformer output end face. Based on Eq. (4), the smaller the cross section of output end, the more energy density is, and the greater amplitude can be obtained.

3. **Machining Experiment**. In the ultrasonic compound electronic machining system shown in Fig. 8, the main device consists of the following elements: ultrasonic generator, ultrasonic vibration device, tool electrode and workpiece, table, pulse power, synchronous power chopper, laser micro displacement sensor, TBS1154 digital storage oscilloscope, and the control computer.

3.1. ***Single Ultrasonic Machining***. It was found that the ultrasonic machining is particularly appropriate for processing hard, brittle, nonmetallic materials such as certain ceramics, glass, gems, etc. Figure 9 shows the processing of nonconductive ceramic PZT by single ultrasonic machining. As is seen, high efficiency, precision and surface quality can be attained. This technology is used in the manufacturing of high-precision piezoelectric sensors.

Fig. 8. Ultrasonic compound electronic machining system graph.

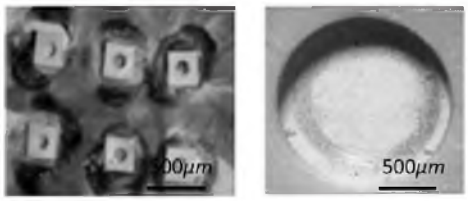

a b

Fig. 9. Ultrasonic machining specimen: (a) ceramic; (b) F2.8 circular hole.

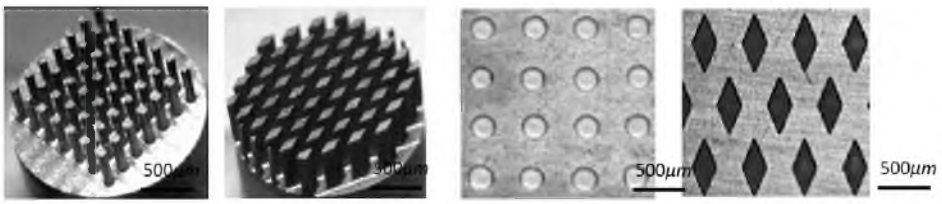

a b c d

Fig. 10. Microelectrode array and machining surface: (a) circular microelectrode; (b) rhombus microelectrode; (c) circular micropits; (d) rhombus micropits.

3.2. ***Ultrasonic Modulation Compound Electric Machining***. The array microstructures (micropits, slightly raised) with shape rules in the friction-pair working surfaces can store oil and produce the liquid lubricating film between the moving surfaces. Using the microelectrode shown in Fig. 10, the processing conditions were as follows: 50 W ultrasonic power, pulse power frequency of 5000 Hz, B4C–W5 power-mixed sodium nitrate aqueous solution with electrolyte of 5%, static pressure of 2 N, processing time of 3 min, chosen materials were YG8, and the ultrasonic modulation compound electrical machining was used as the method. As can be observed, the micro-pits shape, dimensional accuracy, and surface quality are good.

Conclusions

1. The refined ultrasonic vibration test system can provide highly reliable, accurate, and prompt measurements (as proven by the tests).

2. The experiment and mathematical analysis implied that the ultrasonic vibration system amplitude at the output end and the input excitation voltages were approximately linear and proportional independent of the ultrasonic transformer connection to the tool head.

3. The processing tests confirmed that the ultrasonic machining is the efficient method for brittle material processing. The ultrasonic compound electric machining makes it

possible to obtain some microstructures on the surface of the friction pairs that are composed of different materials and had various shapes.

Acknowledgments. The study is supported by the National Natural Science Foundation of China (51375428) and Jiang Su Province Micro-fine Manufacturing Key Lab. The authors thanks for the two funding organizations.

1. F. G. Cao, *Ultrasonic Machining Technology*, Chemical Industry Press, Beijing (2014).
2. Y. W. Zhu, J. Shao, N. Su, and N. Z. Yun, "Research on micro electro-discharged & electrolysis machining technology modulated by synchronizing ultrasonic vibrating," *J Mech. Eng.*, **50**, No. 1, 185–192 (2014).
3. M. R. Shabgard and H. Alenabi, "Ultrasonic assisted electrical discharge machining of Ti–6Al–4V alloy," *Mater. Manuf. Process.*, **30**, No. 8, 991–1000 (2015).
4. J. Shao, Y. Zhu, H. Chen, et al., "Dynamic analysis of ultrasonic compound machining system and microstructure processing," *J. Chem. Pharm. Res.*, **5**, No. 9, 381–387 (2013).
5. Y. F. Chen and Y. C. Lin, "Surface modifications of Al-Zn-Mg alloy using combined EDM with ultrasonic machining and addition of TiC particles into the dielectric," *Mater. Process. Technol.*, **209**, No. 9, 4343–4350 (2009).
6. X. Q. Zhan and H. Qian, "The research of a rotary ultrasonic vibration system," *J. Vibr. Shock*, **29**, No. 4, 218–221 (2010).
7. S. Lin, J. Hu, and Z. Fu, "Electromechanical characteristics of piezoelectric ceramic transformers in radial vibration composed of concentric piezoelectric ceramic disk and ring," *Smart Mater. Struct.*, **22**, No. 4, 045018 (2013).
8. Y. W. Zhu, Z. Wang, Z. J. Fan, et al., "Ultrasonic combined electrical micro-machining technology and its application," *J Mech. Eng.*, **43**, No. 6, 186–197 (2010).
9. X. P. Xie, A. Tian, Z. Wang, and X. C. Yin, "Dynamical performance of ultrasonic stepped horn with loading," *J. Vibr. Shock*, **31**, No. 4, 157–161 (2012).
10. Y. W. Zhu, J. Shao, and H. Z. Chen, "Dynamic analysis and test study of ultrasonic compound micro-fine electrical-machining system," *J Chem. Pharm. Res.*, **5**, No. 8, 126–132 (2013).
11. H. Zarepour, S. H. Yeo, P. C. Tan, and E. Aligiri, "A new approach for force measurement and workpiece clamping in micro-ultrasonic machining," *Int. J. Adv. Manuf. Tech.*, **53**, 517–522 (2011).
12. Y. J. Choi, K. H. Park, Y. H. Hong, et al., "Effect of ultrasonic vibration in grinding; horn design and experiment," *Int. J Precis. Eng. Man.*, **14**, No. 11, 1873–1879 (2013).
13. S. E. Kvashnin and A. A. Maximov, "Effects of heating of deformation antinode areas on amplitude–frequency characteristics of an ultrasonic vibration system," *Biomed. Eng.*, **47**, No. 1, 46–49 (2013).
14. C. Heise, S. Böhm, S. Schwarte, et al., "Hybrid cutting of granite by use of ultrasonic assistance," *Prod. Engineer.*, **8**, No. 5, 567–575 (2014).
15. C.-G. Zhang, Y. Zhang, and F.-H. Zhang, "Mechanism of ultrasonic-pulse electrochemical compound machining based on particles," *J. Centr. South Univ.*, **21**, No. 1, 151–159 (2014).

Received 30. 08. 2016